Origin of Regioselectivity in the *O*-Methylation of Erythromycin as Elucidated with the Aid of Computational Conformational Space Search

Hitoshi Gotō,[a] Yutaka Kawashima,[b] Masato Kashimura,[b] Shigeo Morimoto[b] and Eiji Ōsawa*[,c]
[a] *Department of Chemistry, Faculty of Science, Hokkaido University, Kita-ku, Sapporo 060, Japan*
[b] *Research Center, Taisho Pharmaceutical Co. Ltd., Yoshino-cho Ohmiya, Saitama 330, Japan*
[c] *Department of Knowledge-Based Information Engineering, Toyohashi University of Technology, Tempaku-cho, Toyohashi 441, Japan*

Contrasting regioselectivities reported in the *O*-methylation of 2',4''-bis(*O*-trimethylsilyl)erythromycins (preferentially at 11-OH for the erythromycin A **2**, but almost exclusively at 6-OH for the erythromycin B **3** and the 9-allyloxyiminoerythromycin A **4**) have been studied with the aid of a computational conformational space search technique. Low-energy conformers were exhaustively generated for the model erythronolides **5** (ENA), **6** (ENB) and **7** (ENA oxime) using a new algorithm (CONFLEX) coupled with MM2 geometry-optimization. Hundreds of conformers thus generated were classified into clusters based on the conformation of the 14-membered lactone ring. Examination of stable conformers in the more abundant 17 clusters revealed key features relevant to the *O*-methylation reaction: the orientation of α-hydrogen atom at C(11) and the network of internal hydrogen bonds that occur among hydroxy groups at C(6), C(11), C(12), and carbonyl groups at C(1), C(9). Clusters were then merged according to these reactivity criteria into three bundles; '6-OH reactive', '11-OH reactive' and 'inactive'. The trend in the combined populations in these bundles agree with the observed regioselectivity in the *O*-methylation reaction.

Progress in the computational methods for searching conformational space of cyclic systems[1-9] has made it possible to produce all of the significantly populated conformers for such a large and flexible molecule as cyclotetradecane,[6] cyclohexadecane[10] and cycloheptadecane[3,7] within reasonable computer time. Recent inclusion of capabilities for handling acyclic structures[8,9] allows us to extend the low-energy conformation search technique to large cyclic structures having chain substituents such as naturally occurring macrolide antibiotics.

The macrolide conformation is an old topic,[11] but still remains virtually unresolved due to experimental as well as theoretical difficulties in handling mobile molecules of this size. Take, for example, erythromycin, one of the most well-known antibiotics.[12] Studies based on NMR and CD spectra[13-15] have indicated that the macro-ring of erythromycin exists almost exclusively in a single conformation identical with that of the crystal,[16] in equilibrium with those differing in the C(5) to C(9) segment. More recent studies which combine X-ray analysis with NMR techniques[17] suggest that the aglycone rings of some erythromycin analogues exist as a mixture of a crystal and a 'fold-in[17] [C(7) inward][15]' conformation. No systematic computational conformation search has been described except in a poster session.[18]

An interesting problem on the erythromycin conformation emerged during our chemical modification study to produce clarithromycin **1**, a recently marketed antibiotic having remarkably high oral bioavailability.[19,20] The purpose of the synthetic work was to achieve *O*-methylation with high regioselectivity at 6-OH of erythromycins **2**–**4**, while protecting only the hydroxy groups in the sugar units. Direct methylation of these substrates with methyl iodide in dimethylsulfoxide–tetrahydrofuran (DMSO–THF) (1 : 1) mixed-solvent produced puzzling results (Scheme 1): sugar-protected erythromycin A **2** gave the undesired 11-*O*-methyl ether as the major product, but the similarly protected erythromycin B **3** and 9-allyloxyimino-erythromycin A **4** gave predominantly the desired 6-*O*-methyl ether.[19]

What is the cause of this interesting reversal of selectivity? It apparently depends on the remote substituents at C(9) and C(12). A previous MNDO study[21] on the ease of deprotonation and the stability of anion states of **2** and **3** used only the crystal conformation, hence could not provide a convincing explanation of the regioselectivity. It seems more likely that the difference in the ring substituents among **2** to **4**

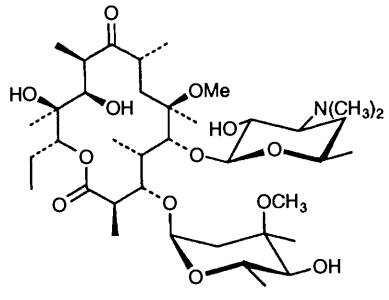

6-*O*-methylerythromycin A (1, Clarithromycin)

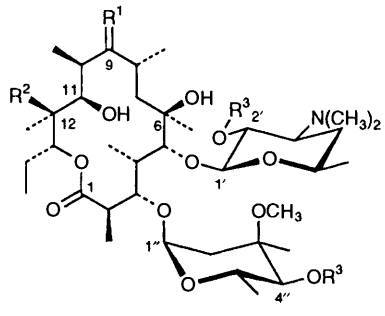

Cmpd.	R^1	R^2	R^3	Selectivity 6-OMe : 11-OMe
2	O	OH	$Si(CH_3)_3$	1 : 3
3	O	H	$Si(CH_3)_3$	> 10 : 1
4	*N*-*O*-allyl	OH	$Si(CH_3)_3$	> 10 : 1

Scheme 1

Table 1 Conformers and clusters found by CONFLEX search

	ENA 5		ENB 6		ENA oxime 7	
	a	*b*	*a*	*b*	*a*	*b*
No. conformers	274	769	182	449	230	679
No. conformation clusters[c]	56	134	41	92	41	99

[a] Conformers within 8 kcal mol^{-1} from the global energy-minimum. [b] Conformers within 10 kcal mol^{-1} from the global energy-minimum. [c] Threshold conformational distance is 10°. For both *a* and *b*, an energy window of 10 kcal mol^{-1} is used for clustering; see text.

might have produced significant effects on the distribution of reactive conformations. If so, this problem can be addressed by the computer conformation search.

This paper describes the results of analysis by the use of the conformation search program CONFLEX. The search produced hundreds of conformers differing in the ring conformation as well as in the rotation of side chains. In order to cope with the large mass of data, we first classified conformers into clusters based on the common ring conformation and then merged the clusters as the analysis progressed.

Computation

Erythronolides **5** (ENA), **6** (ENB) and **7** (ENA oxime) are used to model **2** to **4**, respectively, and these are subjected to the CONFLEX calculations[8,9] using MM2(91)[22] as the energy-minimizer. The molecular mechanics scheme takes care of hydrogen bonding interactions by modified van der Waals parameters.[23] Ring portions are perturbed by bond flip and corner flap to generate new ring conformations, while stepwise rotations (± 120°) are applied to ethyl, methoxy and hydroxy side-chain groups to generate new rotamers. These three types of perturbations are given systematically on the starting geometry.[8,9] Conformers up to 8 kcal mol^{-1} from the global energy minimum have been searched using the reservoir-filling algorithm mentioned elsewhere.[8].

Input structures have been prepared by introducing or removing appropriate functional groups on a tetradecanolide ring constructed from the endocyclic dihedral angles reported for the crystal structure of erythromycin A hydroiodide dihydrate,[16]

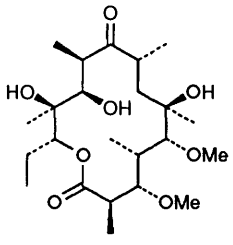

3-*O*,5-*O*-Dimethylerythronolide A
(**5**, ENA)

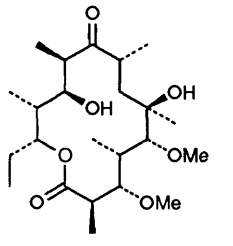

3-*O*,5-*O*-Dimethylerythronolide B
(**6**, ENA)

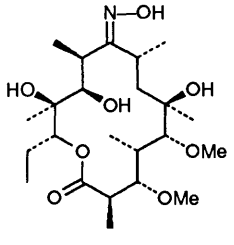

9-Deoxo-9-hydroxyimino-
3-*O*,5-*O*-dimethylerythronolide A
(**7**, ENA oxime)

using the standard values of bond lengths and valence angles. The oxime parameters of Schnur and Dalton[24] are adopted for **7**. Configurations around the C=N and CN–OH bonds of **7** are fixed at *E* and *trans*, respectively.[17]

Results

Clustering.—Table 1 presents the total number of geometry-optimized conformers found within 10 kcal mol^{-1} from the respective global energy-minima of model structures **5**–**7**. We were first struck by the enormous number of conformers found. Actually, these conformers included isomers arising from the rotation of side-chains on the same ring conformation of 14-membered lactone. A number of common ring conformations are found among different models **5**–**7**. These features indicate that the ring conformation may well be used as the first criterion for classifying conformers. When we attempted to use the recently modified Dale's ring nomenclature[25] for grouping conformers, however, too many clusters were produced. Instead, we chose to use 'conformational distance' of the ring atoms as the criterion. Conformational distance (unit in degrees) is defined as the root-mean-square differences in the corresponding torsion angles along the backbone ring between the two conformations being compared.[4,25] Threshold distance, below which the pair of conformers being compared are judged to have the same ring conformation, was chosen to be 10° after several tests. At this resolution, a moderate number of clusters were obtained with the dihedral angles along the ring atoms remaining invariant within the same cluster but significantly differing among different clusters.

To state briefly, our new clustering algorithm consists of the following steps.[26]

1. The *i*-th conformer belongs to cluster A.
2. The conformational distance between the *i*-th and *j*-th conformer is computed.
3. If the distance is smaller than the threshold value (10°), the *j*-th conformer is registered in cluster A, otherwise in cluster B.
4. Steps 2 and 3 are applied to all possible pairs of conformers.
5. The energy level of a cluster is represented by that of the most stable conformer.
6. A check for the duplications. If a conformer is registered in more than one cluster, remove all of them except for the one in the lowest-energy cluster.

The clustering operation mentioned above does not necessarily guarantee that all the conformer pairs within a cluster have conformational distances smaller than the threshold value. For example, if an intermediate conformer *k* exists which is separated from both *i* and *j* by distances within the threshold value, then the conformer *k* and all the conformers in cluster B merge to cluster A (energy A < B).

The clustering efficiency based on this algorithm is strongly influenced by the range of energy. For example, if the conformer *k* mentioned above is 9 kcal mol^{-1} above the global energy minimum (GEM), clusters A and B are independent because we are concerned with an energy range between GEM and 8 kcal

mol^{-1} therefrom. However, if the range is expanded to 10 kcal mol^{-1} from the global minimum, cluster **B** will be swallowed into cluster A. In this work, we studied both cases. For the reasons mentioned above, the latter energy range gave smaller numbers of clusters.

Simple and Boltzmann-weighted averages of endocyclic dihedral angle values in some of the clusters are shown in Table 2 with average deviations within the cluster. From the difference between simple and weighted averages of dihedral angles and their deviations, we note that ring bonds in the conformers of clusters B [C(2)–C(3), C(4)–C(5) and O-C(1)] and D [C(1)–C(2) and C(13)–O] are more flexible than those of clusters A and K.

We then find that only a few of the clusters are meaningfully populated, and that these populated clusters are represented by a very few outstanding conformers. Clusters can be conveniently characterised by three indices: the size, the relative steric energy of the most stable conformer within each cluster (Rel. *E*) and the sum of Boltzmann distribution (Dist.). These indices are given for the ten most stable clusters of each model molecule **5**–**7** in Table 3. 17 Different clusters are entered in this Table and given with arbitrary symbols A to Q.* Table 3 reconfirms the prevailing assumption that erythromycin exists in a very small number, only one or two, conformations in various media.[12]

Cluster A is the most abundant in all the model molecules used. Actually, this ring conformation has appeared in the crystal of erythromycin A.[16] We also find cluster E to be similar to the Demarco conformation.[13] The previously reported 'fold-in [C(7) inward]' conformation appears in a surprisingly high energy region: the 73rd cluster in ENA, the 47th in ENB, and the 40th in ENA oxime, which lie *ca.* 8 kcal mol^{-1} above the respective global minimum.

According to our calculations, we need to consider at most two ring conformations for erythromycin aglycones **5**–**7** in the vapour phase. Note also that ENA **5** is significantly richer in variations of backbone ring conformations compared to other models.

Energy levels of some of the more stable clusters of Table 3 are illustrated in Fig. 1. This Figure reveals an intriguing variation in the relative stabilities of clusters. For example, cluster B is the second most stable of ENA, but is destabilized by 3.2 kcal mol^{-1} by removing 12-OH to give ENB, and much more so by replacing C(9)-carbonyl with an oxime group to give ENA oxime (not given in Fig. 1). Energies of clusters D, E, K and L (the last two not given in Table 3) in ENA are remarkably influenced by removal of 12-OH to give ENB or by introduction of oxime group at C(9) to give ENA oxime. We can anticipate even at this stage of analysis that specific functional groups attached to the lactone ring seem to exert considerable control over the conformer distribution, and perhaps reactivity as well.

Putative Conformational Analysis.—The reactivity of an alcohol in the *O*-methylation under basic condition must be influenced by the acidity of alcohol,[27] which in turn is primarily determined by the stability of the intermediate alkoxide anion[28] as well as by the ease of deprotonation. The alkoxide stability is governed by solvation, which is controlled by the size of α-substituents. Hence a secondary hydroxy group such as 11-OH should be more reactive than a tertiary hydroxy group such as 6- and 12-OH. However, the solvation at 11-OH is also influenced by the conformation around C(11). As can be seen in the ORTEP drawing[29] of the most stable ENA conformer of cluster A (Fig. 2), α-hydrogen atom at C(11) is directed towards the inside of the backbone ring, thus rendering the otherwise open side of the *C*-oxide group inaccessible to solvent molecules. Therefore in cluster A, the 11-OH is expected to behave like tertiary alcohol. Fig. 3 depicts a contrasting picture: in the most stable of the ENA/cluster B conformers, the α-hydrogen atom at C(11) is directed out of the ring and induced ready solvation at the 11-O^- group.

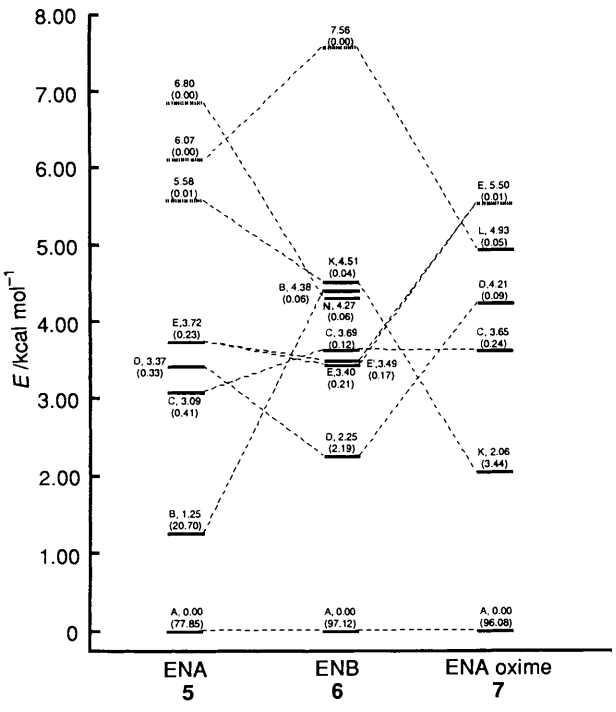

Fig. 1 Energy levels of conformation clusters in ENA **5**, ENB **6** and ENA oxime **7**. Clusters are designated by A to L, each containing unique ring conformation. Numbers correspond to relative steric energy of the most populated conformer in the cluster and those in parentheses the combined Boltzmann distributions of the cluster. Solid horizontal bars pertain to low-energy clusters, while bars denoted by broken lines are entered in the Figure in order to show their correlation with their low-energy relatives in other model structures.

These drawings (Figs. 2 and 3) also show that there are an abundance of internal hydrogen bonds among hydroxy, keto and ester groups at C(1), C(6), C(9) C(11) and C(12). These interactions are probably overestimated in our vapour phase calculations, but they persist in solution according to an NMR study which reveals intramolecular hydrogen bonds in **2** even in polar solvents.[30] Computed geometries indeed reveal a network of hydrogen bond interactions within and along the macrocyclic lactone ring of low-energy conformers.

The second factor that affects the reactivity of alcohols in the *O*-methylation, namely the ease of deprotonation, depends critically upon the intramolecular hydrogen bonding. For example, in the ENA/cluster A conformer of Fig. 2, the hydrogen atom of 12-OH is strongly bound by the oxygen atom of 11-OH, forming a five-membered chelate ring. The hydrogen of 11-OH group is firmly held between C(1)- and C(9)-carbonyl oxygen atoms, seemingly forming a bifurcated hydrogen bond interaction.* It is therefore highly unlikely that the C(11)–O

* A complete table of endocyclic dihedral angles, relative steric energies and Boltzmann distributions of all conformers are given in Supplementary Material (Supp. Pub. No. 56957, 25 pp.). For details of the Supplementary Publication Scheme, see 'Instructions for Authors,' *J. Chem. Soc., Perkin Trans. 2*, 1993, issue 1.

* Note that the hydrogen bond interaction in MM2(91) is not given any directionality. Hence the stability of bifurcated hydrogen bond is probably overestimated.

Table 2 Average endocyclic dihedral angles and their deviations in some of the conformation clusters of erythronolide **5**–**7**[a]

	ENA/Cluster A				ENA/Cluster B				ENB/Cluster D				ENA oxime/Cluster K					
Bond	Av.	Dev.	Boltz. av.	Boltz. dev.	Av.	Dev.	Boltz. av.	Boltz. dev.	Av.	Dev.	Boltz. av.	Boltz. dev.	Av.	Dev.	Boltz. av.	Boltz. dev.	X-ray[b] (fold-out)	X-ray[c] (fold-in)
1–2	120.8	8.7	120.0	2.0	130.2	20.6	147.8	3.4	93.9	15.3	86.7	7.1	130.5	6.6	138.6	2.6	115.9	79.9
2–3	−57.5	4.3	−60.6	0.7	−103.0	23.2	−83.7	10.1	−136.7	6.6	−132.8	2.6	−65.5	3.7	−66.0	0.9	−61.2	−130.8
3–4	157.0	6.6	160.4	1.5	143.0	8.2	137.3	2.7	168.6	10.0	174.3	2.3	147.9	4.2	144.4	1.8	164.8	173.6
4–5	−107.1	9.0	−103.8	2.9	−95.2	10.8	−103.2	8.0	−66.0	5.2	−68.3	1.5	−104.9	5.3	−110.4	2.3	−116.1	−100.1
5–6	−72.9	5.4	−73.4	2.1	−69.5	4.0	−67.6	2.8	−60.0	3.9	−63.6	1.2	−72.0	3.4	−70.0	1.8	−68.5	−60.0
6–7	167.7	4.6	167.0	1.0	146.2	2.6	146.3	1.8	178.4	2.1	176.9	0.8	163.4	3.2	162.5	1.2	175.0	148.0
7–8	−69.8	3.8	−69.1	1.0	−70.3	1.1	−70.4	0.7	−62.2	2.7	−61.4	0.8	−131.0	4.5	−126.6	1.2	−77.0	178.9
8–9	−72.4	2.2	−74.9	0.7	173.2	4.0	178.2	3.6	−84.2	3.5	−82.9	1.1	112.1	2.0	113.1	0.7	−60.8	−53.9
9–10	122.5	5.2	122.2	1.4	−162.9	4.1	−166.8	3.4	94.6	3.2	97.1	1.3	−62.4	2.7	−62.5	1.0	122.0	97.2
10–11	−171.1	4.9	−173.7	1.4	66.6	1.5	65.2	1.1	−177.6	3.6	−178.6	0.9	−134.4	9.8	−142.3	2.3	−173.3	−164.0
11–12	170.1	3.1	171.0	0.8	−135.2	2.8	−133.3	2.0	−175.1	1.9	−174.2	1.0	−173.5	2.7	−176.1	1.1	167.8	165.6
12–13	−66.3	8.2	−60.0	2.2	61.6	3.8	58.6	2.3	−54.7	2.1	−54.4	0.6	−63.3	5.7	−61.6	1.5	−68.6	−70.1
13–O	98.3	4.8	96.6	1.5	105.2	21.2	89.7	2.4	135.5	8.4	139.2	6.2	108.8	5.3	108.4	1.5	107.3	144.6
O–1	171.2	3.6	168.8	1.0	176.2	11.2	165.6	5.2	−163.8	2.8	−164.7	0.6	169.4	2.4	171.3	0.9	171.3	−177.9

[a] Dihedral angle data of other clusters are given in the Supplementary Material. [b] Erythromycin A hydroiodide dihydrate (ref. 16). [c] (*E*)-11-*O*-(2-Dimethylaminoethoxy)methyl-9-deoxo-9-methoxyiminoerythromycin A (ref. 17).

Table 3 Important conformation clusters in erythromycin derivatives

	ENA **5**				ENB **6**				ENA oxime **7**			
No.	Cluster	Size	Rel. E^a	Dist.[b]	Cluster	Size	Rel. E^a	Dist.[b]	Cluster	Size	Rel. E^a	Dist[b]
1	A	77	0.00	77.85	A	51	0.00	97.12	A	112	0.00	96.08
2	B	81	1.25	20.70	D	15	2.25	2.16	K	107	2.06	3.44
3	C	17	3.09	0.41	E	10	3.40	0.21	C	24	3.65	0.24
					E'[c]	8	3.44	0.17				
4	D	14	3.37	0.33	C	4	3.69	0.12	D	22	4.21	0.09
5	E	24	3.72	0.23	N	26	4.27	0.06	L	40	4.93	0.05
6	F	22	3.91	0.18	B	11	4.38	0.06	P	18	4.96	0.03
7	G	13	3.99	0.11	K	26	4.51	0.04	I	7	5.31	0.01
8	H	14	4.41	0.05	O	6	5.04	0.01	Q	9	5.38	0.01
9	I	23	5.10	0.01	M	9	5.43	0.01	H	8	5.41	0.01
10	J	12	5.23	0.01	J	18	5.48	0.01	E	17	5.50	0.01

[a] kcal mol^{-1}. [b] Sum of Boltzmann distribution in %. [c] Cluster E' is close to cluster E, the nearest conformational distance being 11.5°.

bond will rotate from this tightly bound situation to expose its hydroxy proton to a base. On the other hand, the hydrogen atom of 6-OH in Fig. 2 is directed upward from the average ring plane to the open space, hence it should be more susceptible to deprotonation.

Based on considerations mentioned above, we conclude that, in ENA/cluster A conformation, the secondary 11-OH is less acidic than the tertiary 6-OH group. In view of the strong internal hydrogen bond involving the 12-OH groups, the 6-OH appears to be the only available reaction site in the *O*-methylation of conformers belonging to cluster A.

Conformers of cluster B (*e.g.*, Fig. 3) occupy 21% of the whole population in ENA, but it is only marginally populated in both ENB and ENA oxime (Table 3). Cluster B has several notable characteristics. First, the C(9)–carbonyl group falls into the inside of backbone ring, a feature which explains why this conformation is so unfavourable for ENA oxime **7** where in a bulky C=N–O–H group replaces the carbonyl group. Second, it is not the 11-OH proton as in cluster A but the 12-OH proton that is engaged in strong hydrogen bonding interactions with C(9)-carbonyl oxygen atom within the ring. This proton also interacts with C(1)-ester oxygen. Third, the proton of 6-OH group is bound to C(9)- and C(1)-carbonyl oxygen. Hence *O*-methylation of 6- as well as 12-OH must be difficult, whereas the 11-OH group is free to be methylated in the opposite side of the ring plane. Combined with the favourable solvation at C(11) as mentioned above, *O*-methylation of the cluster B conformer will exclusively take place at 11-OH group.

Having studied cluster A, the common global minimum in the three model structures **5**–**7**, and cluster B, the second most stable cluster of ENA, we should mention the second most stable clusters of ENB, namely D, and the corresponding cluster of ENA oxime, K. These are depicted in Figs. 4 and 5, respectively. The ENB conformers belonging to cluster D are similar to those of cluster A in that the 11-OH proton is engaged in strong hydrogen bonding with C(9)-carbonyl oxygen, while 6-OH is free, its O–H bond pointing upward from the average ring plane. There is no 12-OH group in ENB. The cluster K apparently acquired the second largest abundance in ENA oxime because this is one of the few conformations having C(9)-substituent pointing outside the ring. Neither the 6- nor 11-OH group seems available for *O*-methylation, both being held tightly by C(1)-carbonyl oxygen in the inside of ring. The 12-OH is also unreactive, because its proton is strongly held by the 11-OH oxygen forming a five-membered hydrogen bond-ring.

After having performed similar analyses as given above for other clusters appearing in Table 3, we realized that clusters A to Q can be categorized into three bundles with regard to the reactivity in *O*-methylation on the basis of the direction of α-hydrogen at C(11) and the internal hydrogen bond network (Fig. 6). The largest bundle contains clusters which should be preferentially methylated at 6-OH ('6-OH reactive' or $6 > 11$), while the second largest bundle will be predominantly methylated at 11-OH ('11-OH reactive' or $6 \ll 11$) and contains clusters B, I and L. Clusters K, N and P form the smallest, 'inactive' or '6-OH reactive' bundle. Fig. 6 contains simplified drawings of clusters which emphasize orientations of the relevant functional groups.

According to MM2 calculations, the tertiary 12-OH proton in the relatively stable conformers given in Table 3 is always strongly bound, either with the 11-OH oxygen as in clusters A, D and K, or with C(1)- and C(9)-carbonyl oxygen as in cluster B. These features agree well with the experimental fact that under the reaction conditions employed (Scheme 1), no 12-OMe product has been isolated.

Discussion

Distribution of the major cluster bundles within each model structure is given in Fig. 7. For all models, more than 99% of the conformers belong to either one of three bundles. For ENB and ENA oxime, the bundle distributions agree perfectly well with the observed regioselectivity: the '6-OH reactive' and 'inactive' bundles populate more than 99.9%. Qualitatively, the 21% population of the '11-OH reactive' bundle, which appears only in ENA, explains the dominant formation of the 11-OMe product, because of the much-higher reactivity of the secondary 11-OH group compared to the tertiary 6-OH.

The balance among stable conformers is likely to change in the actual reaction conditions from what is predicted above. Especially susceptible to the presence of DMSO will be the hydrogen bond network within the lactone ring. Furthermore, the sugar parts of erythromycin, which are simply replaced with methyl groups in our models **5**–**7**, will exert certain influences on the conformation of the aglycone ring, like polar solvent molecules in unusually close vicinity. No information has so far been available concerning the likely orientation of the sugar groups relative to erythromycin aglycone.

Recently **2** was found to exist as a tautomeric mixture with 6,9- and 9,12-cyclic hemiacetal in highly polar solvents.[30,31] In the DMSO–THF (1:1) mixed-solvent as used here, the equilibrium concentration of the 6,9-hemiacetal is about 5%,[30] and this feature should contribute, if not significantly, to the preferential *O*-methylation at 11-OH.

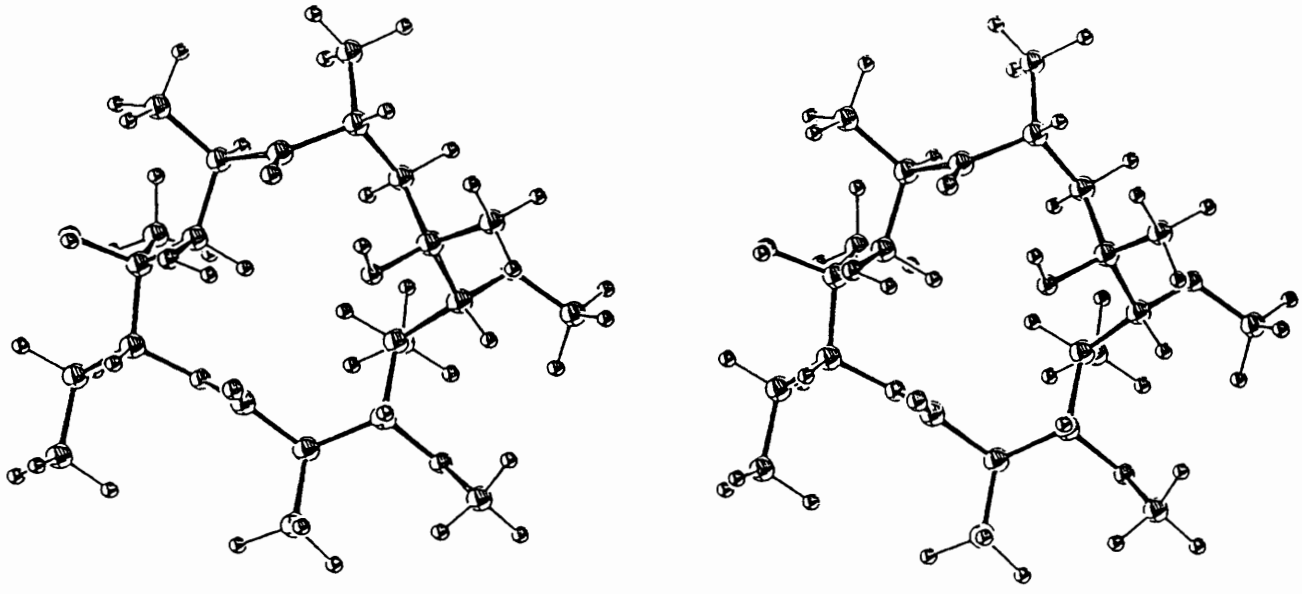

Fig. 2 ORTEP stereo drawing of the most stable conformer in cluster A of erythronolide A (**5**, ENA). Cluster A represents the most stable ring conformation in **5**–**7**.

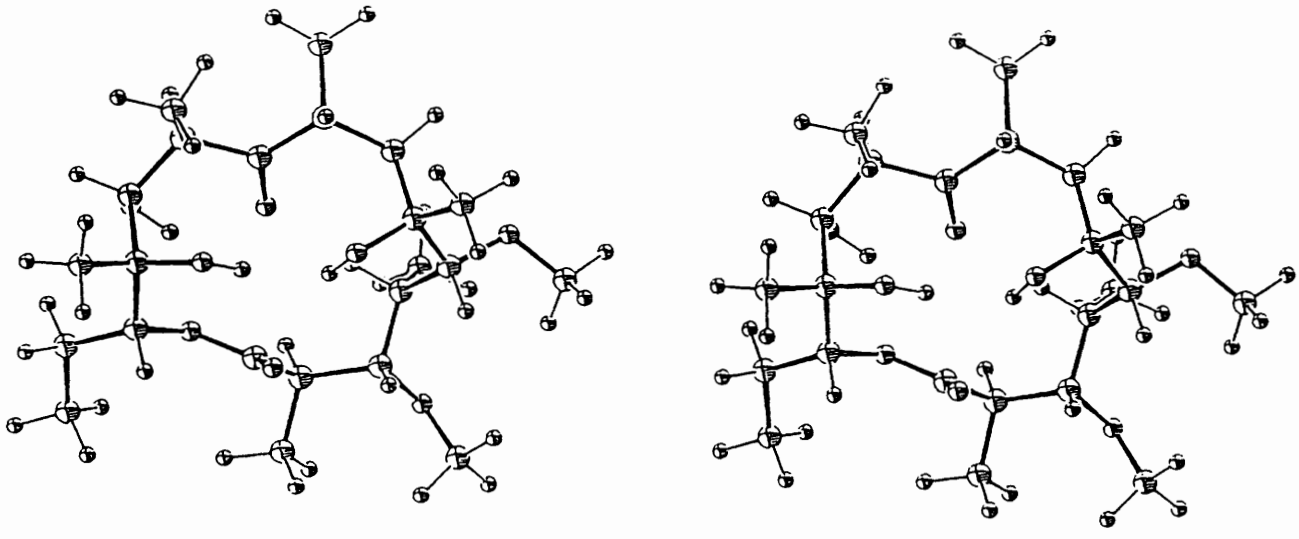

Fig. 3 ORTEP stereo drawing of the most stable conformer in cluster B of erythronolide A (**5**, ENA). Cluster B is virtually non-existent in ENB **6** and ENA oxime **7**.

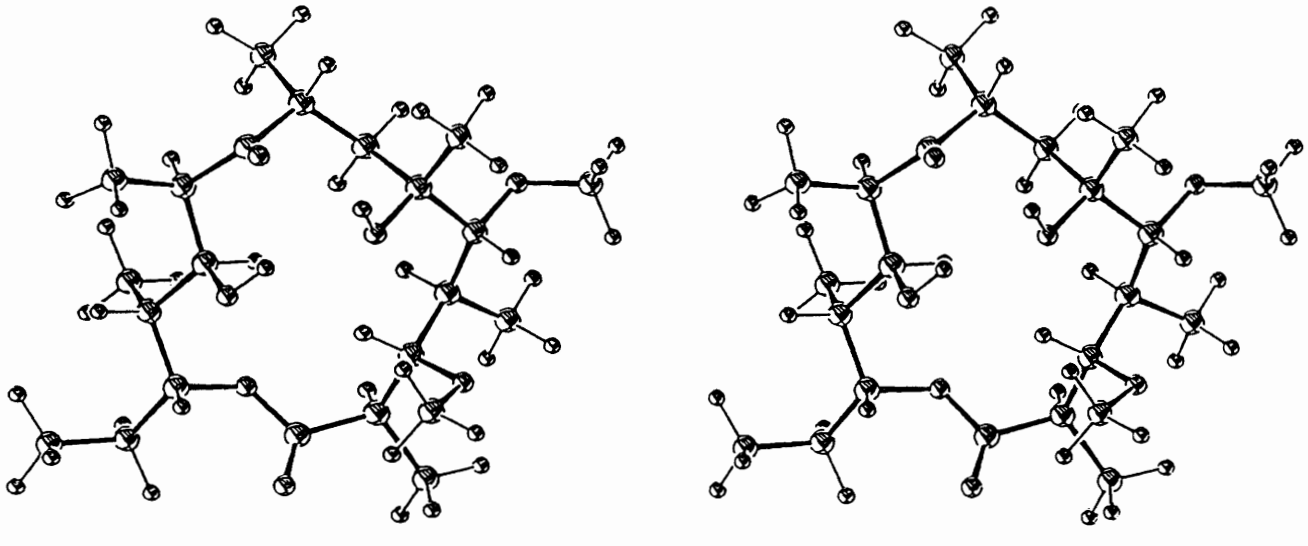

Fig. 4 ORTEP stereo drawing of the most stable conformer in cluster D of erythronolide B (**6**, ENB). Cluster D is the second most populated in ENB **6**.

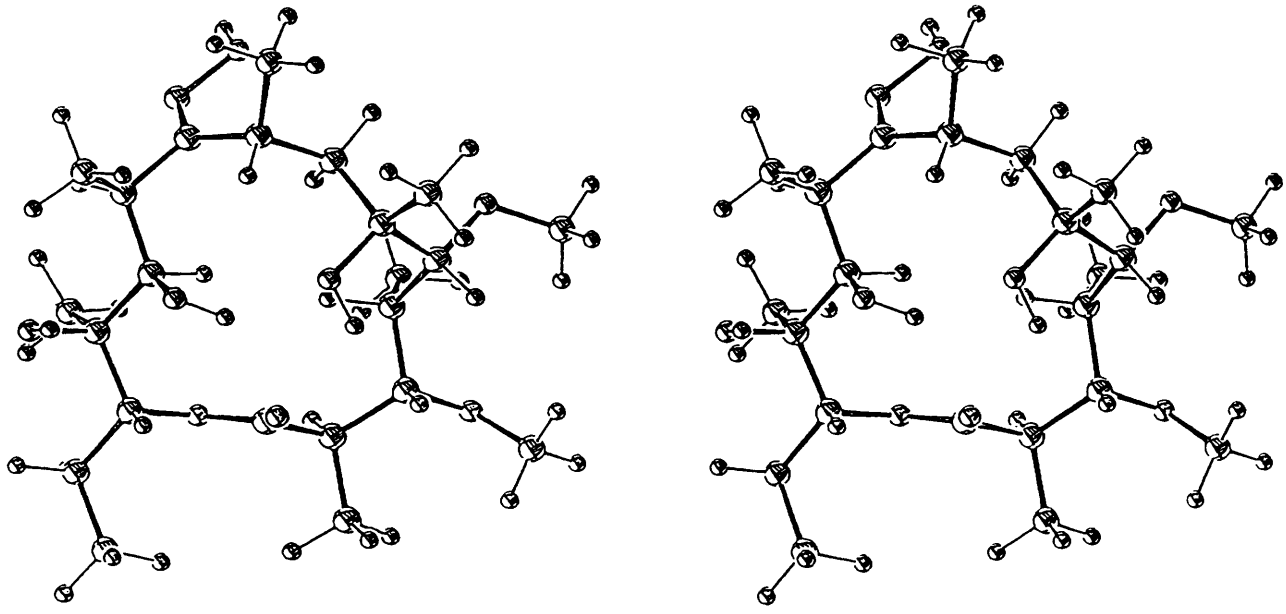

Fig. 5 ORTEP stereo drawing of the most stable conformer in cluster K of erythronolide A oxime (**7**, ENA oxime). Cluster K is the second most abundant in ENA oxime **7**.

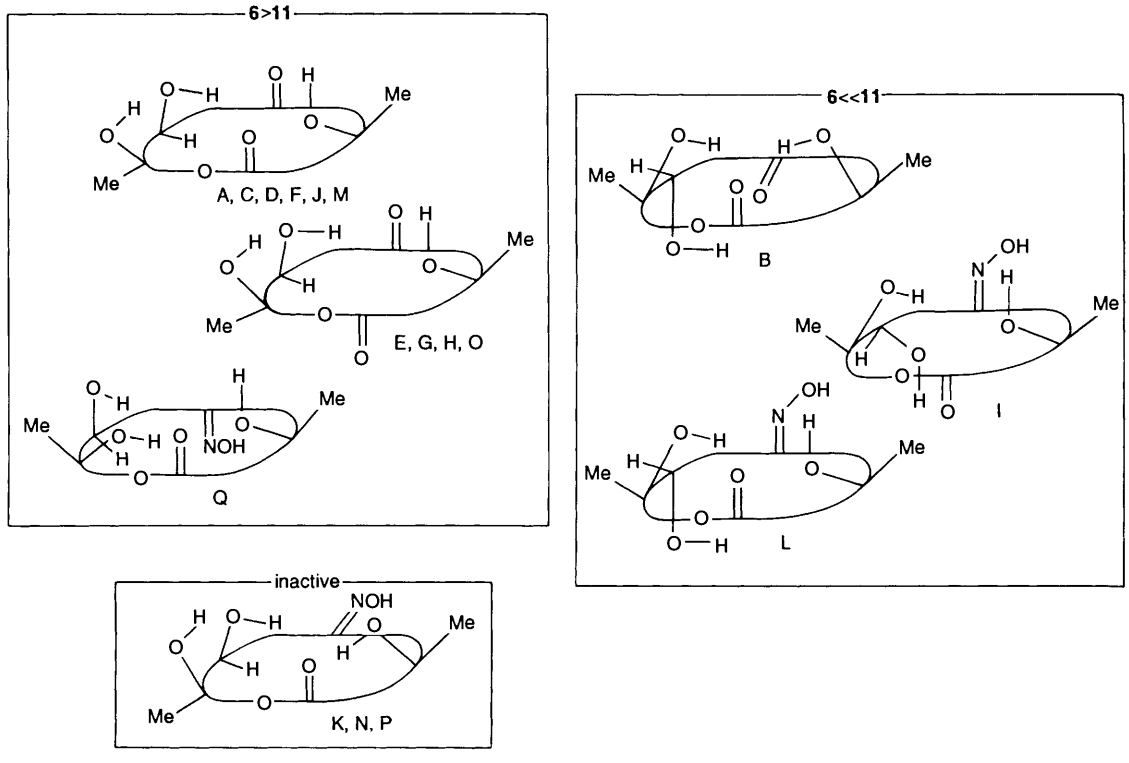

Fig. 6 Three bundles of conformation clusters A–Q. Conformers in the two major bundles are reactive towards *O*-methylation, but should show different regioselectivities. A minor bundle should be unreactive in *O*-methylation.

Acknowledgements

Partial financial support from the Ministry of Education, Science and Culture through a Grant-in-Aid for Scientific Research (No. 03554020) is gratefully acknowledged. H. G. is the holder of a Fellowship for Japanese Junior Scientists from the Japan Society for the Promotion of Science.

References

1 P. A. Kollman and K. M. Mertz, Jr., *Acc. Chem. Res.*, 1990, **23**, 246.
2 H. Gotō and E. Ōsawa, *J. Mol. Struct. (Theochem)*, in the press.
3 M. Saunders, K. N. Houk, Y.-D. Wu, W. C. Still, M. Lipton, G. Chang and W. C. Guida, *J. Am. Chem. Soc.*, 1990, **112**, 1419.
4 M. Saunders, *J. Comput. Chem.*, 1991, **12**, 645.

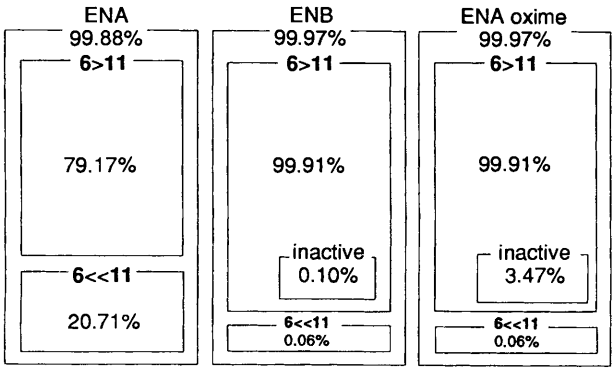

Fig. 7 Calculated populations of three conformation bundles: 6-OH reactive (6 > 11), 11-OH reactive (6 ≪ 11) and inactive

5 H. Gotō and E. Ōsawa, *J. Am. Chem. Soc.*, 1989, **111**, 8950.
6 H. Gotō, M. Shinagawa and E. Ōsawa, manuscript in preparation.
7 H. Gotō and E. Ōsawa, *Tetrahedron Lett.*, 1992, **33**, 1343.
8 H. Gotō and E. Ōsawa, *J. Chem. Soc., Perkin Trans. 2*, 1993, 187.
9 H. Gotō, E. Ōsawa and M. Yamato, *Tetrahedron*, 1993, **49**, 387.
10 H. Gotō and E. Ōsawa, manuscript in preparation.
11 S. Masamune, G. S. Bates and J. W. Corcoran, *Angew. Chem.*, 1977, **89**, 602.
12 J. R. Everett and J. W. Tyler, *J. Chem. Soc., Perkin Trans. 1*, 1985, 2599; *J. Chem. Soc., Chem. Commun.*, 1987, 815; *J. Chem. Soc., Perkin Trans. 2*, 1987, 1659; 1988, 325; see also J. Mulzer, *Angew. Chem., Int. Ed. Engl.*, 1991, **30**, 1452.
13 P. V. Demarco, *J. Antibiot.*, 1969, **22**, 327.
14 T. J. Perun and R. S. Egan, *Tetrahedron Lett.*, 1969, 387; L. A. Mitscher, B. J. Slater, T. J. Perun, P. H. Jones and J. R. Martin, *Tetrahedron Lett.*, 1969, 4505; R. S. Egan, T. J. Perun, J. R. Martin and L. A. Mitscher, *Tetrahedron*, 1973, **29**, 2525; S. Ōmura, A. Neszmélyi, M. Sangré and G. Lukacs, *Tetrahedron Lett.*, 1975, 2939; J. G. Nourse and J. D. Roberts, *J. Am. Chem. Soc.*, 1975, **97**, 4584.
15 R. S. Egan, J. R. Martin, T. J. Perun and L. A. Mitscher, *J. Am. Chem. Soc.*, 1975, **97**, 4578.
16 D. R. Harris, S. G. McGeachin and H. H. Mills, *Tetrahedron Lett.*, 1965, 679.
17 J. R. Everett, I. K. Hatton, E. Hunt, J. W. Tyler, D. J. Williams, *J. Chem. Soc., Perkin Trans. 2*, 1989, 1719; E. Hunt and J. W. Tyler, *J. Chem. Soc., Perkin Trans. 2*, 1990, 2157; J. R. Everett, I. K. Hatton and J. W. Tyler, *Magn. Reson. Chem.*, 1990, **28**, 114.
18 K. H. Kim, Y. C. Martin, E. T. Olejniczak and S. Harrod, a poster presented in the 1987 Gordon Conference on Computational Chemistry, New Hampshire, USA.
19 S. Morimoto, Y. Takahashi, Y. Watanabe and S. Omura, *J. Antibiot.*, 1984, **37**, 187; S. Morimoto, Y. Misawa, T. Adachi, T. Nagate, Y. Watanabe and S. Omura, *J. Antibiot.*, 1990, **43**, 286; S. Morimoto, T. Nagate, K. Sugita, T. Ono, K. Numata, J. Miyachi, Y. Misawa, K. Yamada and S. Omura, *J. Antibiot.*, 1990, **43**, 295; Y. Watanabe, T. Adachi, T. Asaka, M. Kawashima and S. Morimoto, *Heterocycles*, 1990, **331**, 2121.
20 A. B. Jones, *J. Org. Chem.*, 1992, **57**, 4361.
21 Y. Kawashima, S. Morimoto, T. Matsunaga, M. Kashimura, T. Adachi, Y. Watanabe, K. Hatayama, S. Hirono and I. Moriguchi, *Chem. Pharm. Bull.*, 1990, **38**, 1485.
22 U. Burkert and N. L. Allinger, *Molecular Mechanics*, American Chemical Society, Washington, DC, 1982.
23 N. L. Allinger, R. A. Kok and M. R. Imam, *J. Comput. Chem.*, 1988, **10**, 591. For a more recent implementation of H-bond in MM2, see S. A. Vazquez, M. A. Rios and L. Carballeira, *J. Comput. Chem.*, 1992, **13**, 851.
24 D. M. Schnur and D. R. Dalton, *J. Org. Chem.*, 1988, **53**, 3313.
25 H. Gotō, *Tetrahedron*, 1992, **48**, 7131.
26 H. Gotō, manuscript in preparation.
27 R. T. Morrison and R. N. Boyd, *Organic Chemistry*, Allyn and Bacon, Newton, Massachusetts, 1983.
28 E. M. Arnett and K. E. Molter, *Acc. Chem. Res.*, 1985, **18**, 339; E. M. Arnett, *J. Chem. Educ.*, 1985, **62**, 385.
29 C. K. Johnson, ORTEP-II: A Fortran Thermal-Ellipsoid Plot Program for Crystal Structure Illustrations, Report ORNL-5138, Oak Ridge National Laboratory, Oak Ridge, TN, USA, 1976. A PC version was used and output directly onto a laser printer (CANON LBP-406B); ORTEP-PC98, Y.-M. Xun and E. Ōsawa, JCPE No. P032 and also ORTEPC Rev. 1.04, J. Toyota, JCPE No. P039.
30 J. R. Everett, E. Hunt and J. W. Tyler, *J. Chem. Soc., Perkin Trans. 2*, 1991, 1481.
31 J. Barber, J. I. Gyi, L. Lian, G. A. Morris, D. A. Pye and J. K. Sutherland, *J. Chem. Soc., Perkin Trans. 2*, 1991, 1489; J. Barber, J. I. Gyi, G. A. Morris, D. A. Pye and J. K. Sutherland, *J. Chem. Soc., Chem. Commun.*, 1990, 1040; J. I. Gyi and J. Barber, *Biochem. Soc. Trans.*, 1991, **19**, 313.

Paper 3/02017G
Received 7*th April* 1993
Accepted 14*th May* 1993